IJE TRANSACTIONS B: Applications Vol. 39, No. 05, (May 2026) 1254-1266

International Journal of Engineering

Journal Homepage: www.ije.ir

Numerical Evaluation of Behavior of Tapered Piled Raft in Loose Sand

M. S. Shokoohfar, M. Khanmohammadi*

Department of Civil Engineering, Isfahan University of Technology, Isfahan, Iran

P A P E R I N F O

Paper history:
Received 21 April 025
Received in revised form 19 May 2025
Accepted 04 July 2025

Keywords:
Piled Raft
Tapered Pile
Bearing Capacity
Finite Element
Settlement

A B S T R A C T

Tapered piles, with a larger diameter at the top than at the bottom, provide higher shaft resistance than conventional cylindrical piles and may offer a more economical alternative. Adding piles to a raft foundation improves its bearing capacity and reduces settlement. While tapered piles have been investigated for decades, limited research has focused on tapered piled raft systems. This study evaluates the behavior of piled rafts incorporating tapered and cylindrical piles of varying lengths and configurations in sandy soil. The model includes a raft measuring 15 × 15 × 0.7 meters, and piles with an average diameter of 1 meter. The taper angle of 1.20 degrees results in top diameters of 1.25, 1.376, and 1.502 meters and bottom diameters of 0.75, 0.624, and 0.498 meters for pile lengths of 12, 18, and 24 meters, respectively. A 3D finite element model was developed using PLAXIS 3D. Multiple simulations were performed with various pile types and arrangements. The model was validated against three experimental studies, confirming its reliability. Results show that tapered piles offer greater shaft resistance than cylindrical piles. Central piles carry less load compared to edge and corner piles. Increasing the number of piles reduces differential settlement. Additionally, tapered piled rafts demonstrated lower differential settlement than cylindrical piled rafts, highlighting their effectiveness in enhancing overall performance.

doi: *10.5829/ije.2026.39.05b.17*

Graphical Abstract

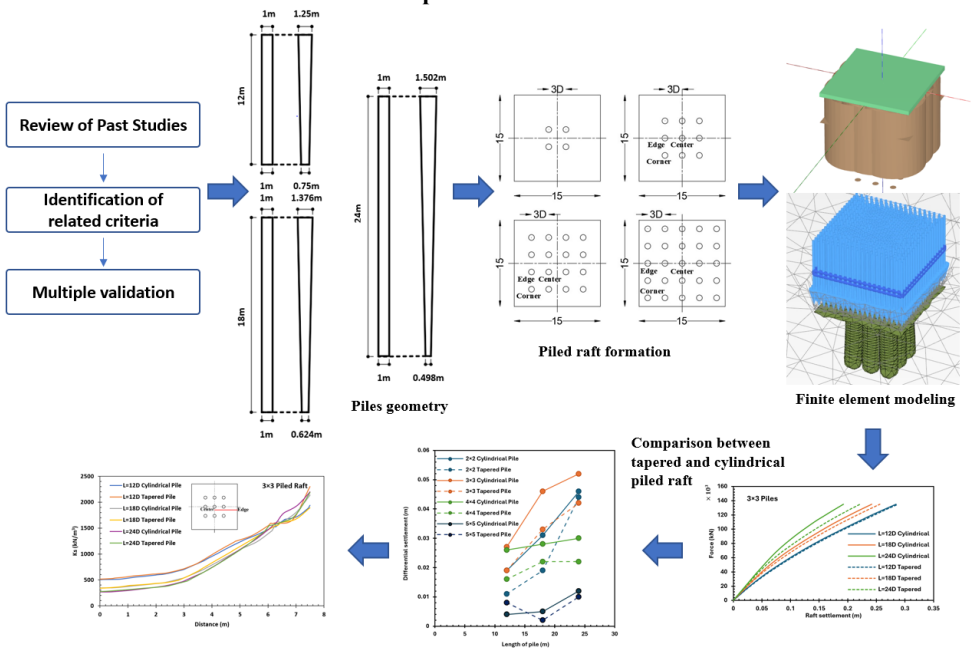

*Corresponding Author Email: mkhanmohammadi@iut.ac.ir (M. Khanmohammadi)

Please cite this article as: Shokoohfar MS, Khanmohammadi M. Numerical Evaluation of Behavior of Tapered Piled Raft in Loose Sand. International Journal of Engineering, Transactions B: Applications. 2026;39(05):1254-66.

1. INTRODUCTION

Utilizing piles with raft is considered as a solution when the surface layer of soil does not have the necessary load bearing capacity. Meanwhile, tapered piles with increased shaft bearing capacity can be an ideal option to operate along the raft. Although the group performance of these piles has received the attention of several researchers. However, the utilization of tapered piles beneath the raft and the interaction between them have not been investigated. Therefore, the shortage of research about the group of tapered piles, especially tapered piled rafts, doubles the need to investigate this issue.

Previous studies indicate that tapered piles provide larger shaft bearing than cylindrical piles with equal volume (1-8). The performance of different geometrical parameters on tapered piles has been examined. El Naggar and Wei (5) concluded that the optimal tapered effect is considerable in the depth of 20 times pile diameter (L=20D) in compressive loads. The shaft bearing capacity of tapered piles was evaluated by Khan et al. (6) utilizing experimental and finite element analyses, leading to the conclusion that a greater taper angle increases the shaft resistance. Tavasoli and Ghazavi (7) have conducted experimental and numerical analysis to investigate the drivability of tapered and semi-tapered piles. They concluded that decreasing the pile tip diameter increased both the velocity and the settlement of the piles. El Naggar and Sakr (9) concluded that the length of the tapered piles should not exceed 20 to 25 times the diameter of the pile (L=25D) in order to achieve optimal efficiency.

In the last two decades, experimental research has been done on the tapered pile group (10, 11) and some numerical modelling (12, 13) to investigate the tapered effect on the pile group. Shafaghat et al. (13) extended the pile group efficiency relationship proposed by Sayed and Bakeer (14) to calculate the group efficiency for bored tapered piles.

Randolph (15) proposed three approaches for designing of piled raft. The first is the conventional method where the piles are built to support the majority of the load. The second method, where the piles are built to withstand 70-80% of operational load. The last method is where the piles are utilized to decrease the differential settlement. Research on piled raft foundations mainly includes numerical modelling (16-23) due to the difficulty of conducting experimental studies. However, only a few of these researches have focused on experimental studies (24-26). Sinha and Hanna (21) conducted a numerical study on the performance of the piled raft in cohesive soil. They observed that by increasing the pile spacing up to 6D, the bearing capacity of the piled raft decreases and after that, the raft carries almost the full load of the building. Lee et al. (19) evaluated the response of piled rafts under vertical loading. Their result showed that the loading type (distributed or concentrated) affects load distribution in the pile according to its arrangement in the raft. Luo et al. (27) studied the response of rigid piled rafts in clay soil. They reported that the normal settlement reduces with the increase of the safety factor, they also suggested a safety factor of 3 for the designing of the piled raft. Khanmohammadi and Fakharian (22) analyzed the response of piled rafts with various lengths, spacings, and arrangements. They concluded that increasing the pile length and reducing the pile spacing, decreases the settlement and increases the contribution of piles in load bearing. However, pile spacing for rafts on dense soils has less effect than rafts placed on looser soils. Banerjee et al. (28) have investigated the performance of piled raft in multi-layered soil using finite element analysis. They concluded that to achieve an efficient performance the pile group-raft area ratio is between 0.4 to 0.6. Jeong et al. (29) have investigated piled raft deformation and load distribution using numerical and analytical methods. They concluded that the settlement performance and load distribution of piled raft is reliant on foundation stiffness (pile-raft-soil interaction and raft flexibility).

The load applied to the piled rafts can be transmitted to the soil through the raft or the piles. To determine the effect of piles in the raft and also to determine their load-carrying contribution, the piled raft coefficient is characterized as follows:

$$\alpha = \frac{Q_P}{Q} \quad (1)$$

where Q_P is the part of the load supported by the piles and Q is the total applied load. It is noteworthy that α=0 is equal to a raft without any piles and α=1 is equal to a piled raft where the cap has no interaction with the surface of the soil (and provides no load bearing contribution).

In this study, finite element analysis has been conducted to evaluate the performance of tapered piled raft. The impact of pile length and arrangement for tapered and cylindrical piles has been evaluated.

2. MESHING AND BOUNDARY CONDITIONS

The performance of the tapered piled raft was determined by three-dimensional finite element analysis. PLAXIS 3D (2023) finite element software was chosen for modelling. Figure 1 shows the generated mesh for models. A 10-node tetrahedral elements fine mesh was employed for all models, and by using the coarseness factor for the surfaces of the piles and raft, smaller meshes have been created around the piles and raft than in other parts of the models. A square raft with a width and thickness of 15 meters and 0.7 meters respectively and piles with an average diameter of 1 meter with

various lengths (length to pile diameter ratio of 12, 18, and 24) were positioned in the center of the raft. The piles were modeled using volume elements. This approach allows for accurate modelling of the geometry of both tapered and conventional piles and simulates the pile-soil interaction around the pile circumference. Figure 2 shows the raft geometry and positioning of the piles.

The relative flexibility of the rectangular raft was calculated with the criterion provided by Horikoshi and Randolph (30) which is specified in the following relationship:

$$K_{rs} = 5.57 \frac{E_r(1-v_s^2)}{E_s(1-v_r^2)} \left(\frac{B}{L}\right)^{\alpha} \left(\frac{t_r}{L}\right)^3 \quad (2)$$

where E_r, v_r, E_s and v_s are raft Young's modulus, raft Poisson ratio, soil Young's modulus and soil Poisson ratio respectively, B and L are the lateral and longitudinal dimension of the raft, t_r is the raft thickness and α is aspect ratio. Differential settlement is dependent on the raft aspect ratio (B/L). To minimize this dependency, $\alpha = 0.5$ has been considered. By using the materials properties specified in Table 2 the value of K_{rs} will be equal to 0.575 which represents a flexible piled raft. Raft relative flexibility is important because it directly affects raft center settlement and differential settlement.

Khanmohammadi and Fakharian (31) concluded that the soil in proximity of the pile is affected by pile installation. Therefore, to avoid the influence of model dimensions on finite element analysis, the boundaries considered on each side of the raft are 4 times the length of the raft, and the depth of the model is 8 times the length of the rafts, which results in a cube with dimensions of 135 meters as illustrated in Figure 3. The boundary conditions for the vertical boundaries are (normally fixed), which expresses the freedom of movement in the Z direction, and for the bottom horizontal boundary, boundary conditions are fully fixed.

3. CONSTITUTIVE MODELLING

The behavior of loose sand has been modelled by the Mohr-Coulomb model, and it is expressed as follows:

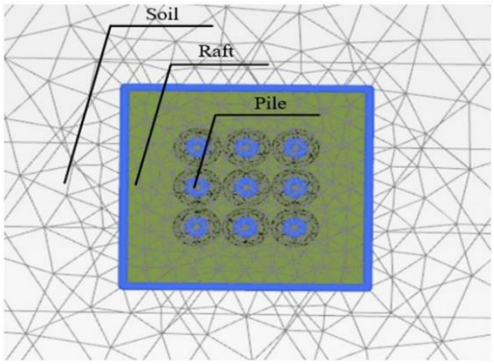

Figure 1. Finite element mesh around the piled

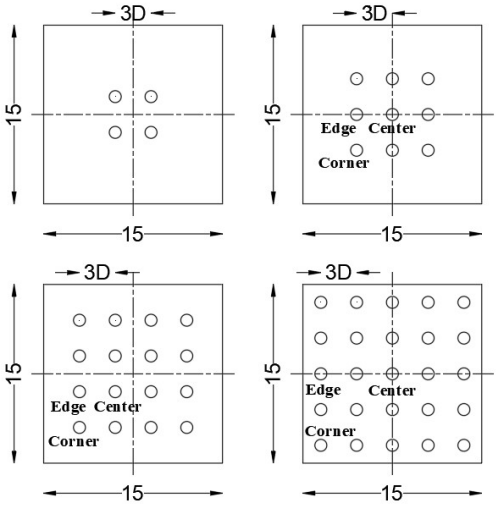

Figure 2. Plies arrangement used in a finite element analysis

$$\tau = c + \sigma \tan\varphi \quad (3)$$

where τ and σ are the shear stress and normal stress at the failure plane, c is cohesion and φ is the soil friction angle. Also, the behavior of concrete used for modelling of piles and raft was modeled through the linear elastic model according to Hooke's isotropic elasticity law. The Mohr-Columb model has also been used to simulate interfaces including soil-raft and soil-piles. The interface element between the soil and the piled raft will cause small displacements and sliding between the two surfaces. The parameters of the interface will be determined using the parameter R_{inter} and it is calculated with the defined parameters of the soil around the interface element as follows (32):

$$c_i = R_{inter} \times c_{soil} \quad (4)$$

$$\tan\varphi_i = R_{inter} \times (\tan\varphi_{soil}) \quad (5)$$

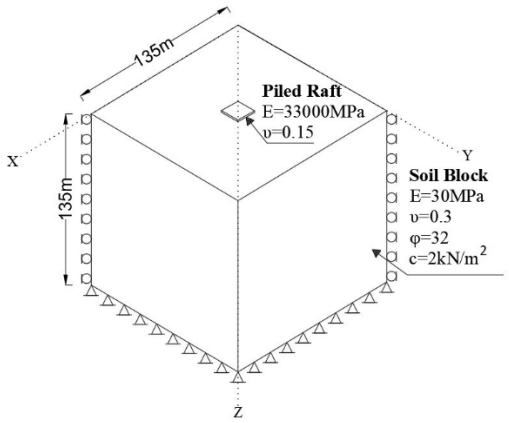

Figure 3. Schematic sketch of the numerical model and boundary condition

where c_i is the cohesion of the interface and φ_i is the internal friction angle of the interface.

The piled raft and the soil were modelled using characteristics described in Table 1. The considered soil is loose sand modelled by the Mohr-Coulomb model. The characteristics of loose sand considered in this study have a good match with values considered for loose sand by Bowles and Guo (33).

A similar value for Rinter has been considered for better comparison with similar studies which is used for validation as well. Additionally, to achieve the precise modelling of the soil-pile interface, the R_{inter} coefficient for sand in contact with concrete considered in this study was compared with the studies of Potyondy (34), Praporgescu and Popa (35) a good match was obtained. The average diameter for all the piles is considered 1 meter and the raft dimensions are 15×15×0.7 and the loading was distributed uniformly on the raft. The cross-sectional area of tapered piles changes linearly from top to bottom (for example, for a 12 meter pile, the cross-sectional area of the pile starts at a diameter of 1.25 meter at the top, reaches 1 m in the middle of the pile, and reaches 0.75 meter at the pile tip). The variables are the number, length, and tapered angle of the piles. The geometric specifications of the models are specified in Table 2.

TABLE 1. Material properties used in finite element analysis

Parameter	loose Sand	Concrete
Material Model	Mohr-Coulomb	Linear Elastic
Unit Weight, γ (kN/m^3)	17	25
Elastic modulus, E(MPa)	30	33000
Poisson's ration, υ	0.3	0.15
Cohesion, C (kPa)	2	-
Friction angle, φ˚	32	-
Dilatancy angle, ψ˚	2	-
R_{inter}	0.95	-

TABLE 2. Geometry properties used in finite element analysis

Model	Pile Formation	L/D	α˚	D_{top}(m)	D_{bot}(m)
1	2×2	12	0˚	1	1
2		18		1	1
3		24		1	1
4		12	1.2˚	1.25	0.75
5		18		1.376	0.624
6		24		1.502	0.498
7	3×3	12	0˚	1	1
8		18		1	1
9		24		1	1
10	4×4	12	1.2˚	1.25	0.75
11		18		1.376	0.624
12		24		1.502	0.498
13		12	0˚	1	1
14		18		1	1
15		24		1	1
16		12	1.2˚	1.25	0.75
17		18		1.376	0.624
18		24		1.502	0.498
19	5×5	12	0˚	1	1
20		18		1	1
21		24		1	1
22		12	1.2˚	1.25	0.75
23		18		1.376	0.624
24		24		1.502	0.498

4. VALIDATION

Validation of three experimental studies on piles (tapered and cylindrical single pile, tapered pile group, and piled raft) have been carried out to ensure the accuracy of modelling for this study. The first validation was done to ensure the correct modelling of tapered piles. Wei and El Naggar (4) investigated the axial performance of two types of tapered piles with tapered angles of 0.6 and 0.95 degrees and cylindrical piles in sandy soil inside a chamber with a diameter of 1.5 meters and a depth of 1.445 meters. For accurate modelling of the confining pressure of the soil, a hardening soil model was utilized. The material characteristics utilized in the validations are shown in Table 3. These findings are correlated with the load-settlement performance acquired from the current finite element study employing PLAXIS 3D, in Figure 4a, and it shows a good match.

To ensure the correct modelling of the interface between tapered piles, a second validation based on Nasrollahzadeh and Hataf's (11) study was used.

They investigated the performance of the tapered pile group in a cubical chamber with dimensions of 1×1×1 m. Piles in two types of tapered (with an angle of 1°) and cylindrical with a buried length of 0.6 meters and an average diameter of 7.3 cm were used. The material characteristics are provided in Table 3. The load settlement performance from experimental research shows good agreement with the graph obtained from numerical modelling in Figure 4b.

Poulos's (36)study was used to validate the accuracy of piled raft performance on sand. Poulos analyzed, employing various software like FLAC 3D and GASP, a

TABLE 3. Model parameters and properties for various materials used for validations

Parameters	Wei and El Naggar (4)	Nasrollahzadeh and Hataf (11)	Poulos (36)
Material Model	Hardening soil	Mohr-Coulomb	Mohr-Coulomb
Unit weight, γ (kN/m^3)	18	17	15.9
Saturated unit weight, γsat (kN/m^3)	20	20	-
Elastic modulus, E (MPa)	-	25	30
Secant stiffness, E50 (MPa)	30	-	-
Tangent stiffness, Eoed (MPa)	30	-	-
Unloading / reloading stiffness, Eur (MPa)	90	-	-
Poisson's ration, υ	0.3	0.35	0.3
Friction angle, φ	35	32	30
Cohesion, C (kPa)	2	4	2
Dilatancy angle, ψ	5	2	0
	Steel Properties	**Concrete Properties**	
Material Model	Linear Elastic	Linear Elastic	
Unit weight, γ (kN/m3)	78.5	24	
Elastic modulus, E(MPa)	2.00E+05	3.00E+04	
Poisson's ration, υ	0.3	0.2	

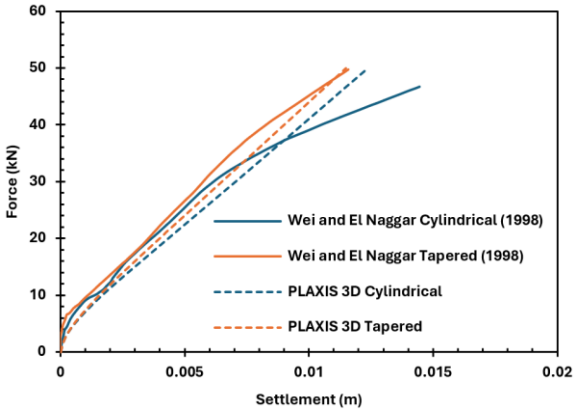

a) load-settlement responses obtained by Wei and El Naggar for single tapered and cylindrical piles.

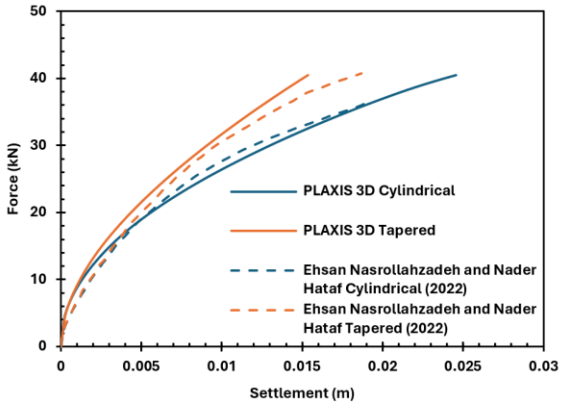

b) Load-settlement responses obtained for tapered and cylindrical pile groups by Nasrullahzadeh and Hatef.

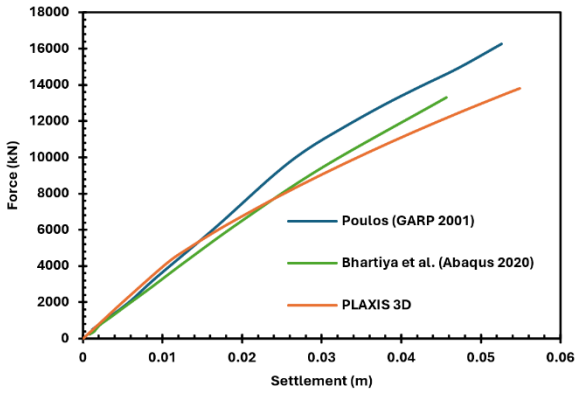

c) Load-settlement responses obtained for piled raft analyzed by Poulos.

Figure 4. Validation of PLAXIS 3D finite element analysis

piled raft supported by 9 piles with the diameter of 0.5 and the length of 10 meters respectively, placed under a raft of 0.5×6×10 meters. Table 3 illustrates the material properties used in this validation. The results show a slight difference in the settlement of the middle of the piled raft between Poulos and the present study. Also, Bhar tiya et al. (37) analyzed the piled raft foundation modelled by Poulos with ABAQUS software. Figure 4c shows the load-settlement performance for Poulos and the present study. The obtained load-settlement response for this study has a good match with the previous results, the slight differences can happen due to various assumptions in the elasto-plastic characteristics of sand.

5. RESULTS AND DISCUSSION

5. 1. Piled Raft Bearing Capacity Figure 5 illustrates the load-settlement response for center of piled rafts with various pile length ratios. As expected, the foundation settlement decreases with a rise in the pile length. This process is evident for all modelled piled rafts with any quantity of piles. Also, with a rise in the number of piles, the settlement of the raft center decreases, which is due to the participation of more piles in the load bearing process. This decrease in settlement is greater for piles with a longer length than piles with a shorter length (which leads to the separation of the load-settlement response for piles with various lengths).

By comparing the tapered and cylindrical piled rafts, it is evident that the tapered angle increases the settlement of the piled rafts. Also, a rise in pile length, causes greater settlement for tapered piled rafts than cylindrical ones.

Figure 6 illustrates the load-settlement performance for the three types of piles according to their position in the raft (center, edge, and corner) for the arrangement of 9, 16, and 25 piled rafts is shown. It can be seen that the tapered and cylindrical piles in the center, edge, and corner undergo more settlement respectively. A similar performance can be seen in piled rafts by raising the quantity of piles from 9 to 16. However, the behavior of the piles is different for the 25 piled rafts. Piles position is inclined to the edge of the raft because of the rise in their number (the piles were positioned in the center of the rafts due to the assumed 3D spacing between piles). This causes the piles to have more interaction with adjacent soil (which is not under direct loading). This increase in interaction for corner piles has come from both sides. Figure 6 shows the diagram of the center, edge, and corner piles for a 25 piled raft. It is clear that unlike the raft with 9 and 16 piles, piles in these positions experience less settlement respectively. Khanmohammadi and Fakharian (22) also concluded similar results by analyzing the load-settlement performance of the 64 piled rafts for the piles in the mentioned position. The ratio of the settlement of the edge and corner piles to the center pile is given in Table 4. In this table, the settlement of the center pile is given in Q_{135MN} column (the settlement for 135 MN loading on the raft), and the settlement ratio of the edge and corner piles with the center pile (in constant loading) is determined.

5. 2. Tapered Effect On Differential Settlement of The Piled Raft The settlement difference between the corner and the center of the piled raft is defined as the differential settlement. The number and arrangement of piles are influential in the differential settlement. A rise in the volume of the piles in the center of the piled raft can lead to a rise in the differential settlement. Depending on the arrangement, geometry, and type of the load applied, a piled raft can experience less center settlement, while the corners of the raft (given their distance from the

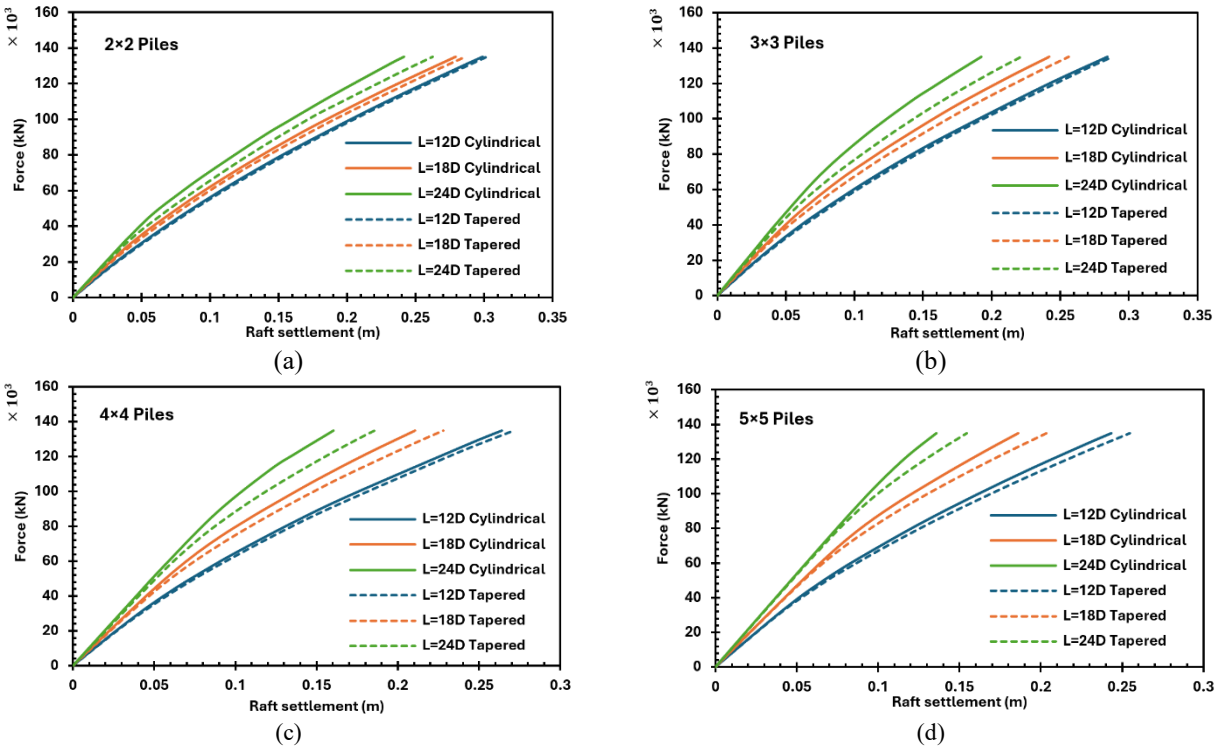

Figure 5. Load-settlement response for the tapered and cylindrical piled raft with a) 4 piles, b) 9 piles, c) 16 piles and d) 25 piles

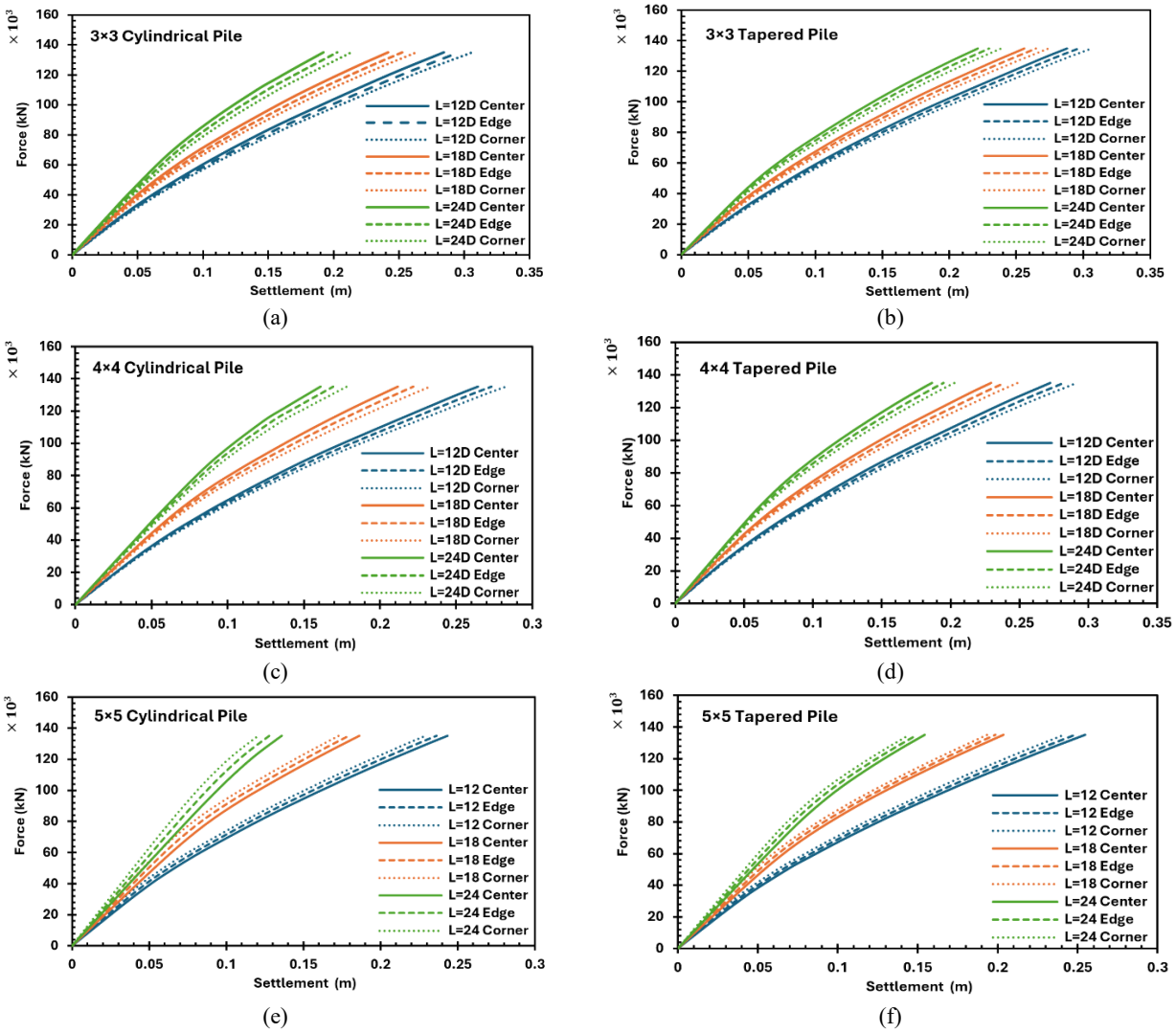

Figure 6. Load-settlement responses for the tapered and cylindrical piled raft for center, edge and corner piles for a) 3×3 cylindrical pile b) 3×3 tapered pile c) 4×4 cylindrical pile d) 4×4 tapered pile e) 5×5 cylindrical pile f) 5×5 cylindrical pile

TABLE 4. Settlement ratio of piles considering their position in raft

Case	Pile Formation	L/D	α°	Q_{135MN}(m)	Q_{edge}/Q_{center}	Q_{corner}/Q_{center}
1	2×2	12	0°	0.299	1	1
2		18		0.279	1	1
3		24		0.242	1	1
4		12	1.2°	0.302	1	1
5		18		0.287	1	1
6		24		0.262	1	1
7	3×3	12	0°	0.284	1.041	1.077
8		18		0.242	1.045	1.089
9		24		0.192	1.054	1.110
10		12	1.2°	0.288	1.030	1.063
11		18		0.256	1.033	1.070
12		24		0.221	1.038	1.079

13	4×4	12	0°	0.264	1.034	1.070
14		18		0.212	1.048	1.099
15		24		0.161	1.051	1.106
16		12	1.2°	0.272	1.035	1.070
17		18		0.229	1.043	1.085
18		24		0.186	1.044	1.088
19	5×5	12	0°	0.243	0.971	0.940
20		18		0.186	0.964	0.929
21		24		0.136	0.940	0.888
22		12	1.2°	0.255	0.976	0.949
23		18		0.204	0.975	0.951
24		24		0.154	0.969	0.939

piles) can experience more settlement, which will lead to differential settlement. Also, a piled raft can experience uniform settlement throughout the piled raft (regardless of the total settlement) by carefully placing the piles in the raft. Figure 7 illustrates that for the piled raft with a small number of piles (4 piles and 9 piles), raising the length of the piles results in an increase in differential settlement, while for more piles, the differential settlement is negligible. It should be mentioned that the differential settlement for the 9 piled raft exceeds the 4 piled raft, which is due to a rise in the volume of the piles and the decrease of the settlement at the center of the raft. Because of the constant distance between piles, increasing the length of the piles leads to a rise in the volume of the piles in a small area beneath the raft, which reduces the settlement, while the settlement in the raft's edges increases in piled rafts with fewer piles. But in the case of more piles and a wider arrangement the differential settlement decreases.

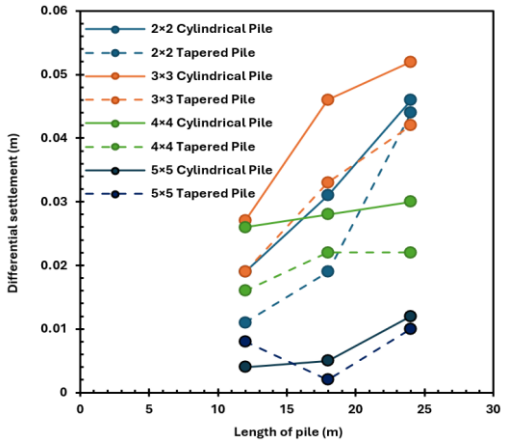

Figure 7. Differential settlement for tapered and cylindrical piled raft

It is also evident that the differential settlement of the tapered piled rafts is less than cylindrical piled rafts, which indicates the positive effect of tapered piles on differential settlement reduction.

5. 3. Tapered Effect on Piled Raft Coefficient The comparison of piled raft coefficient with increasing pile length, for tapered and cylindrical piles is shown in Figure 8. The findings illustrate that the piled raft coefficient increases with a rise in the quantity of the piles, this is because more piles participate in the load bearing and the raft portion of the load decreases. Also, the piled raft coefficient increases with a rise in the length of the piles, which indicates the increase in the shaft bearing capacity of each pile. It is evident that in 25 piled rafts with a rise in pile length from L/D=18 to L/D=24, the piled raft coefficient does not experience a significant increase. Whereas the other piled rafts with relatively lower piled raft coefficients showed more increase. Figure 8 also shows that tapered piles have a lower piled raft coefficient, which is a result of multiple interactions in piled raft foundation.

5. 4. Axial Force In Piles Piles can perform differently considering their position in the raft. Figure 9 to 11 show axial force in tapered and cylindrical piles for center, edge, and corner piles. It is evident that tapered piles have higher shaft bearing capacity at any position than cylindrical piles, which match with previous studies (1, 4, 6).

It is evident that piles located at the center of the raft absorbed lesser loading in comparison with other piles in the raft. This is revealed when the length of piles in the rafts reaches from 12 meters to 18 and 24 meters(according to the quantity of piles in the raft). For example, in Figure 9, with an increase in the pile length from 12 to 18 and 24 meters, it is found that the loading

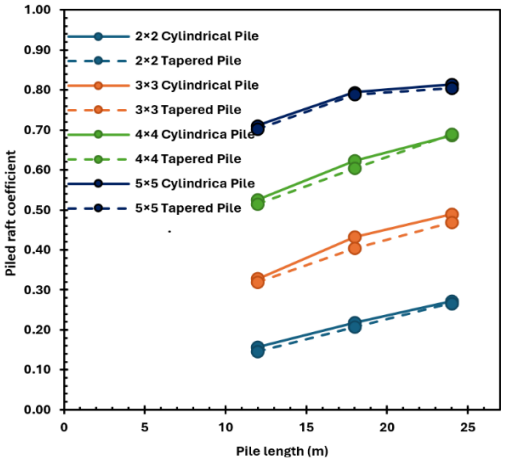

Figure 8. Piled raft coefficient for tapered and cylindrical piled raft

share of piles increases, and it is also observed that the absorbed loading for the center pile has lesser increase than the rest of the piles. Lee et al. (19) indicated that the loading share of the center pile was lower than other piles, which was dependent on the loading level of the piled raft.

According to Figure 9-11, with an increase in pile length for center piles, the axial force remains relatively constant within a specific depth range (no force transition occurs between pile and soil). Figure 12 illustrates the settlement of the center pile and soil with the length of 12 and 24 m for 4×4 piled raft. It is evident that, the neutral plane for piles with no force transition between pile and soil occurs in deeper layers of soil.

Also, tapered piles have lower tip bearing capacity due to the lesser cross section at the pile's toe than cylindrical ones.

The total stress developed in the soil in the cross-section due to the absence of pore water pressure (the groundwater level was considered to be at the lowest possible level) is equal to the effective soil stress. Figure 13 shows a vertical cross-section of a 5×5 piled raft with a length of 12 times the pile diameter, for both tapered

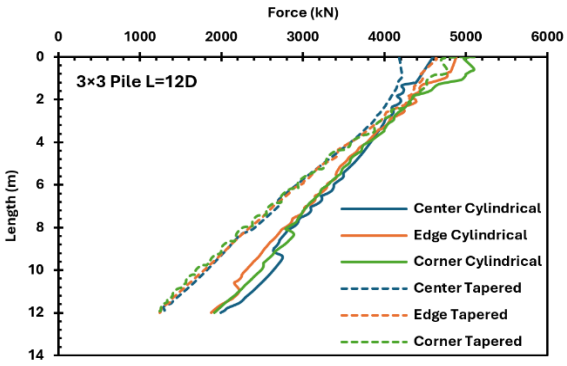

(a)

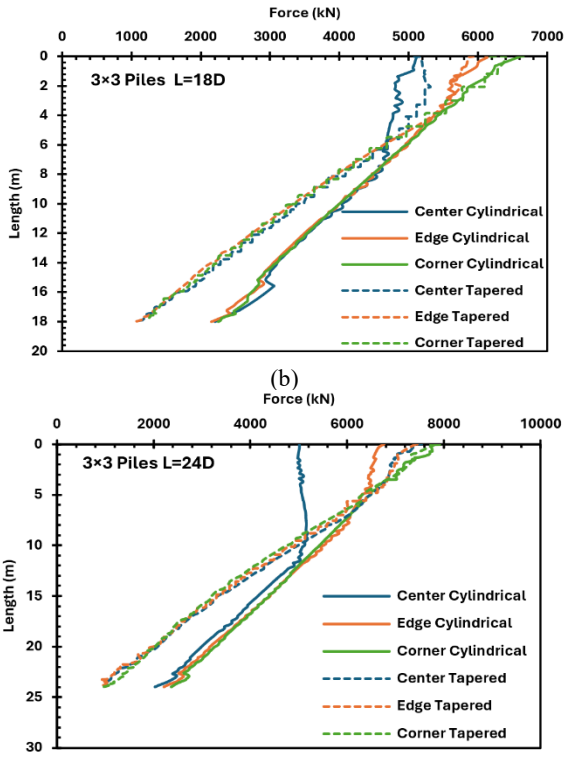

(b)

(c)

Figure 9. Axial force for tapered and cylindrical piles in center, edge and corner of 3×3 Piled raft with a) L=12D b) L=18D c) L=24D

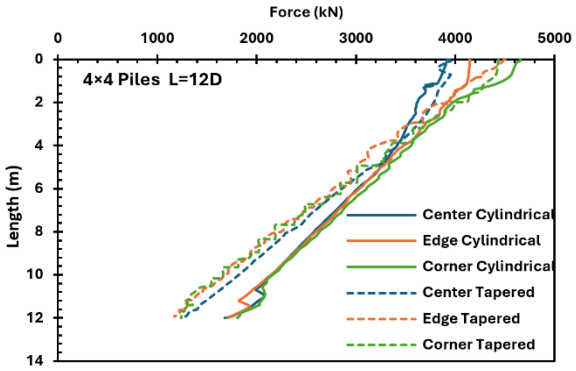

(a)

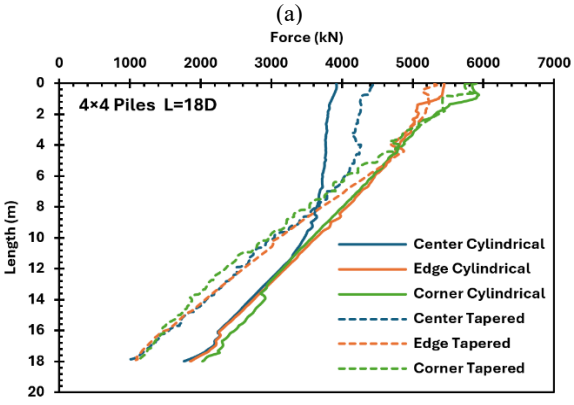

(b)

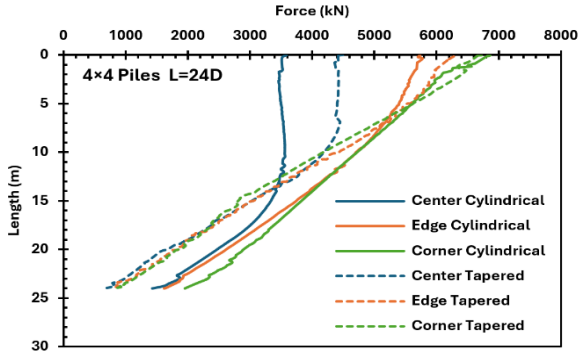

(c)

Figure 10. Axial force for tapered and cylindrical piles in center, edge and corner of 4×4 piled raft with a) L=12D b) L=18D c) L=24D

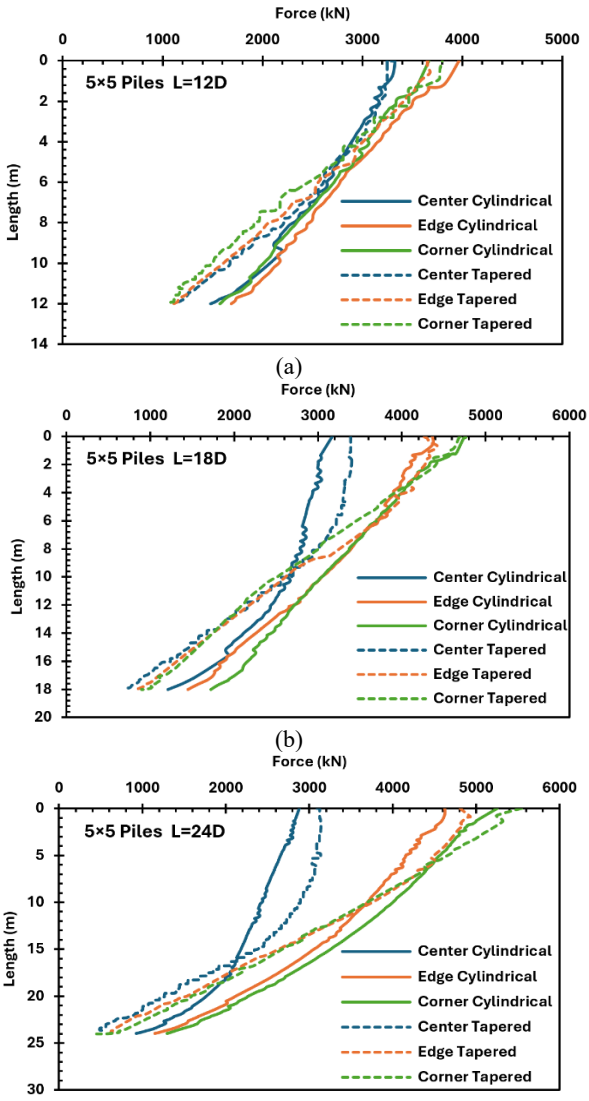

(a)

(b)

(c)

Figure 11. Axial force for tapered and cylindrical piles in center, edge and corner of 5×5 piled raft with a) L=12D b) L=18D c) L=24D

and cylindrical piles. This cross-section, which passes symmetrically through the center of the raft, depicts the stresses resulting from loading and initial soil layer pressure.

According to Figure 13, the stress value under the cylindrical pile tip is -1325 kN/m², while this value reaches -1872 kN/m² for tapered piles. This increase in stress beneath the tapered pile tip is attributed to its smaller cross-sectional area compared to the cylindrical pile (note that part of the stress contour directly under the pile tip has been excluded in the Figure 13 to provide a clearer visualization of the overall stress distribution). It is worth noting that, the stress distribution contour under piles tip is higher for cylindrical piles than the tapered piles beneath the piled raft. On the other hand, the stress distribution contour around the piles shaft shows a greater value for tapered piles.

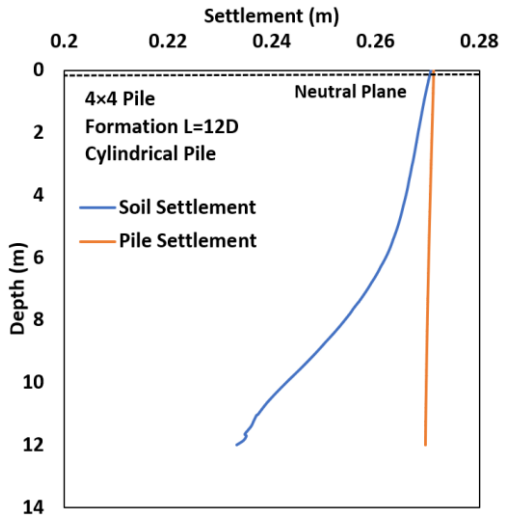

(a)

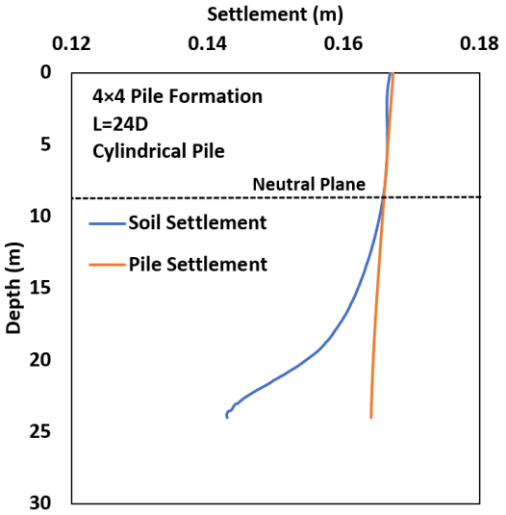

(b)

Figure 12. Illustration of pile-soil settlements and Neutral plane for 4×4 piled raft with a) L=12D b) L=24D

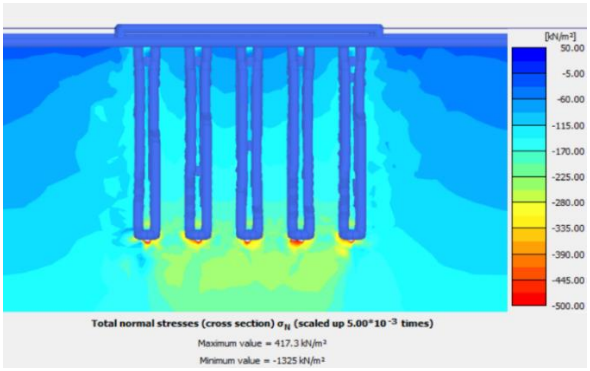

(a)

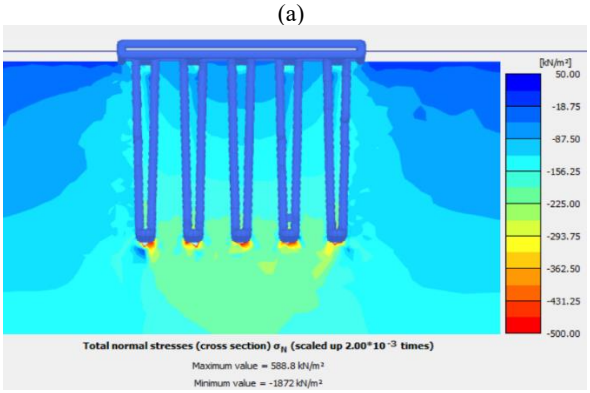

(b)

Figure 13. Stress distribution for 5×5 piled raft for a) cylindrical piles b) tapered piles

5. 5. Soil Subgrade Modulus Soil subgrade modulus is calculated by obtaining the stress and displacement of the soil in the vertical direction. Bowles and Guo have proposed the following equation to calculate K_s (33):

$$K_s = \frac{\Delta\sigma}{\Delta\delta} \quad (6)$$

where $\Delta\sigma$ is the increment of contact pressure and $\Delta\delta$ is the corresponding deformation in the vertical direction.

Figure 14 shows the soil subgrade modulus along the raft (from the center to the side for rafts with different piles). It can be seen that the subgrade modulus does not change much with the change in the pile length, which is in accordance with the observations of Khanmohammadi and Fakharian (22). With an increase in the pile number the magnitude of K_s decreases, but it maintains its increasing trend from the middle to the edge of the raft. As the number of piles in the soil increases, the contact area of the pile with the soil decreases. This has led to a decrease in the soil subgrade modulus. Bhartiya et al. (37) mentioned the K_s ratio of the edge to the center of the raft is equal to 5, which indicates the increasing trend in the mentioned study.

In the present study, this value is equal to 5.8 in its highest state in Figure 13 (for the raft with 9 tapered piles with a length of 24), which is in agreement with the value mentioned by Bhartiya et al. (37) The difference between the present study and the mentioned report is the slope of the graph, in the present study the graph slope is milder than in those cases.

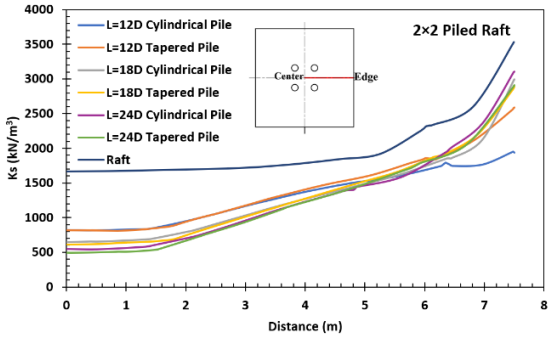

(a)

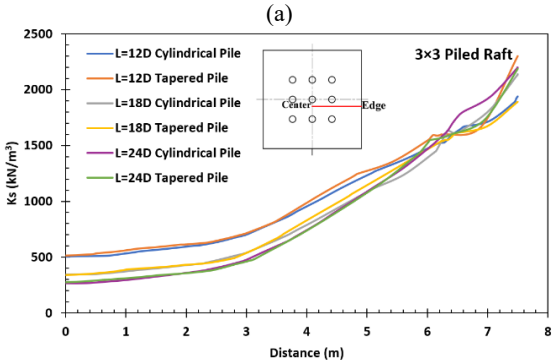

(b)

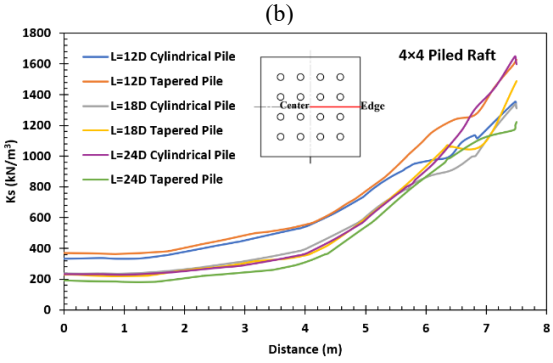

(c)

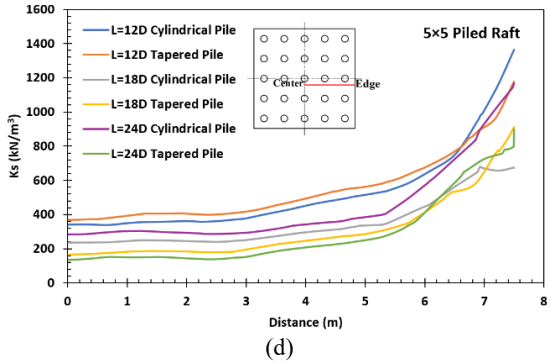

(d)

Figure 13. Soil subgrade modulus for the tapered and cylindrical piled raft in a) 4 piled raft, b) 9 piled raft, c) 16 piled raft and d) 25 piled raft.

6. CONCLUSIONS

In this study, a series of finite element analyses were conducted using PLAXIS 3D software to investigate the effect of tapered angle on piled raft foundations in sandy soil subjected to vertical loading. For this purpose, piles with different numbers and lengths, tapered and cylindrical, were placed at a fixed distance in the center of the raft.

The accuracy of the analyses has been evaluated through multiple validations. The main results obtained are as follows:

- As expected, for both tapered and cylindrical piled rafts, settlements decrease with a rise in length and quantity of piles in a constant loading. Also, it can be seen that the tapered piled rafts have more settlement than cylindrical piled rafts, this becomes clearer when the pile length increases. This increase in settlement is due to stress transmission from the pile to the surrounding soil because shaft bearings generated more widely along the tapered piles.
- By examining the differential settlement of piled rafts, it is evident that rafts with tapered piles have lesser differential settlement compared to cylindrical piles.
- By examining the axial force along cylindrical and tapered piles in raft, it is evident that the tapered piles absorb more of the loading than the cylindrical ones for center piles. Also, it can be seen that tapered piles have larger shaft bearing capacity but smaller end bearing.
- It is obvious from this research that as the quantity of piles increases soil subgrade modulus reduces. It was observed that K_s value increases with a moderated slope from the center of the raft to the edge of the raft.

As it was concluded the settlement of tapered piled rafts is slightly higher than cylindrical piled rafts and it is due to insufficient tip bearing of piles and more contribution of raft. But considering the high shaft bearing capacity, tapered piled rafts promise better performance with floating piles.

7. REFERENCES

1. Robinsky E, Sagar W, Morrison C. Effect of shape and volume on the capacity of model piles in sand. Canadian Geotechnical Journal. 1964;1(4):189-204. https://doi.org/10.1139/t64-015
2. Robinsky E, Morrison C. Sand displacement and compaction around model friction piles. Canadian Geotechnical Journal. 1964;1(2):81-93. https://doi.org/10.1139/t64-002
3. Kodikara JK, Moore ID. Axial response of tapered piles in cohesive frictional ground. Journal of Geotechnical Engineering. 1993;119(4):675-93. https://doi.org/10.1061/(ASCE)0733-9410(1993)119:4(675)
4. Wei J, El Naggar MH. Experimental study of axial behaviour of tapered piles. Canadian Geotechnical Journal. 1998;35(4):641-54. https://doi.org/10.1139/t98-033
5. El Naggar MH, Wei JQ. Axial capacity of tapered piles established from model tests. Canadian Geotechnical Journal. 1999;36(6):1185-94. https://doi.org/10.1139/t99-076
6. Khan MK, El Naggar MH, Elkasabgy M. Compression testing and analysis of drilled concrete tapered piles in cohesive-frictional soil. Canadian Geotechnical Journal. 2008;45(3):377-92. https://doi.org/10.1139/T07-107
7. Tavasoli O, Ghazavi M. Effect of tapered and semi-tapered geometry on the offshore piles driving performance. Ocean Engineering. 2020;201:107147. https://doi.org/10.1016/j.oceaneng.2020.107147
8. Ghazavi M, Lavasan AA, editors. Bearing capacity of tapered and step-tapered piles subjected to axial compressive loading. The 7th international conference on coasts Ports & marine structures, ICOPMAS, Tehran, Iran; 2006.
9. Naggar MHE, Sakr M. Evaluation of axial performance of tapered piles from centrifuge tests. Canadian Geotechnical Journal. 2000;37(6):1295-308. https://doi.org/10.1139/t00-049
10. Shabanpour A, Ghazavi M, El Naggar MH. Behavior of axially loaded tapered pile groups using centrifuge test. Innovative Infrastructure Solutions. 2023;8(6):168. https://doi.org/10.1007/s41062-023-01114-9
11. Nasrollahzadeh E, Hataf N. Experimental and numerical study on the bearing capacity of single and groups of tapered and cylindrical piles in sand. International Journal of Geotechnical Engineering. 2022;16(4):426-37. https://doi.org/10.1080/19386362.2019.1651042
12. Hataf N, Shafaghat A. Numerical comparison of bearing capacity of tapered pile groups using 3D FEM. Geomechanics and Engineering. 2015;9(5):547-67. https://doi.org/10.12989/gae.2015.9.5.547
13. Shafaghat A, Khabbaz H, Fatahi B. Axial and lateral efficiency of tapered pile groups in sand using mathematical and three-dimensional numerical analyses. Journal of Performance of Constructed Facilities. 2022;36(1):04021108. https://doi.org/10.1061/(ASCE)CF.1943-5509.0001680
14. Sayed SM, Bakeer RM. Efficiency formula for pile groups. Journal of geotechnical engineering. 1992;118(2):278-99. https://doi.org/10.1061/(ASCE)0733-9410(1992)118:2(278)
15. Randolph M, editor Design methods for pile group and piled rafts. Proc 13th Int Conf on SFE, 1994; 1994.
16. El-Garhy B, Galil AA, Youssef A-F, Raia MA. Behavior of raft on settlement reducing piles: Experimental model study. Journal of Rock Mechanics and Geotechnical Engineering. 2013;5(5):389-99. https://doi.org/10.1016/j.jrmge.2013.07.005
17. Nguyen DDC, Jo S-B, Kim D-S. Design method of piled-raft foundations under vertical load considering interaction effects. Computers and Geotechnics. 2013;47:16-27. https://doi.org/10.1016/j.compgeo.2012.06.007
18. de Sanctis L, Mandolini A. Bearing capacity of piled rafts on soft clay soils. Journal of Geotechnical and Geoenvironmental Engineering. 2006;132(12):1600-10. https://doi.org/10.1061/(ASCE)1090-0241(2006)132:12(1600)
19. Lee J, Kim Y, Jeong S. Three-dimensional analysis of bearing behavior of piled raft on soft clay. Computers and Geotechnics. 2010;37(1-2):103-14. https://doi.org/10.1016/j.compgeo.2009.07.009
20. Prakoso WA, Kulhawy FH. Contribution to piled raft foundation design. Journal of geotechnical and geoenvironmental engineering. 2001;127(1):17-24. https://doi.org/10.1061/(ASCE)1090-0241(2001)127:1(17)

21. Sinha A, Hanna A. 3D numerical model for piled raft foundation. International Journal of Geomechanics. 2017;17(2):04016055. https://doi.org/10.1061/(ASCE)GM.1943-5622.0000674
22. Khanmohammadi M, Fakharian K. Evaluation of performance of piled-raft foundations on soft clay: A case study. Geomechanics and Engineering. 2018;14(1):43-50. https://doi.org/10.12989/gae.2018.14.1.043
23. Fakharian k, Khanmohammadi M. Evaluation of the effect of geometric characteristics of a piled-raft on its behavior on soft clay under drained conditions. Sharif Journal of Civil Engineering. 2013;29(2):71-6.
24. Fioravante V, Giretti D, Jamiolkowski M, editors. Physical modeling of raft on settlement reducing piles. From research to practice in geotechnical engineering; 2008. https://doi.org/10.1061/40962(325)2
25. Horikoshi K, Matsumoto T, Hashizume Y, Watanabe T, Fukuyama H. Performance of piled raft foundations subjected to static horizontal loads. International Journal of Physical Modelling in Geotechnics. 2003;3(2):37-50. https://doi.org/10.1680/ijpmg.2003.030204
26. Long PD, Vietnam V. Piled raft—a cost-effective foundation method for high-rises. Geotechnical Engineering. 2010;41(1):149. https://doi.org/10.14456/seagj.2010.7
27. Luo R, Yang M, Li W. Normalized settlement of piled raft in homogeneous clay. Computers and Geotechnics. 2018;103:165-78. https://doi.org/10.1016/j.compgeo.2018.07.023
28. Banerjee R, Bandyopadhyay S, Sengupta A, Reddy G. Settlement behaviour of a pile raft subjected to vertical loadings in multilayered soil. Geomechanics and Geoengineering. 2022;17(1):282-96. https://doi.org/10.1080/17486025.2020.1739754
29. Jeong S, Park J, Chang D-w. An approximate numerical analysis of rafts and piled-rafts foundation. Computers and Geotechnics. 2024;168:106108. https://doi.org/10.1016/j.compgeo.2024.106108
30. Horikoshi K, Randolph M. On the definition of raft—soil stiffness ratio for rectangular rafts. Géotechnique. 1997;47(5):1055-61. https://doi.org/10.1680/geot.1997.47.5.1055
31. Khanmohammadi M, Fakharian K. Numerical modelling of pile installation and set-up effects on pile shaft capacity. International Journal of Geotechnical Engineering. 2019. https://doi.org/10.1080/19386362.2017.1368185
32. PLAXIS 3D Reference Manual: bentley; 2023.
33. Bowles JE, Guo Y. Foundation analysis and design: McGraw-hill New York; 1996.
34. Potyondy JG. Skin friction between various soils and construction materials. Geotechnique. 1961;11(4):339-53. https://doi.org/10.1680/geot.1961.11.4.339
35. Praporgescu A, Popa A, editors. Different aspects regarding slope stability improvement using piles. IOP Conference Series: Materials Science and Engineering; 2024: IOP Publishing. https://doi.org/10.1088/1757-899X/1304/1/012009
36. Poulos H. Piled raft foundations: design and applications. Geotechnique. 2001;51(2):95-113. https://doi.org/10.1680/geot.2001.51.2.95
37. Bhartiya P, Chakraborty T, Basu D. Nonlinear subgrade modulus of sandy soils for analysis of piled raft foundations. Computers and Geotechnics. 2020;118:103350. https://doi.org/10.1016/j.compgeo.2019.103350

Persian Abstract

چکیده

رادیه شمع‌ها با انتقال بخشی از بارگذاری از سوی رادیه به خاک، گزینه‌ای اقتصادی‌تر برای تحمل بارهای وارد شده، در مقایسه با دیگر پی‌های شمعی در نظر گرفته می‌شوند. هرچند که افزایش باربری جداری شمع‌های مخروطی در دهه‌های گذشته مورد بررسی قرار گرفته است اما تحقیقات کافی بر عملکرد گروهی این شمع‌ها به خصوص رادیه شمع‌های مخروطی صورت نگرفته است. در پژوهش حاضر رادیه شمعی با شمع‌های مخروطی و استوانه‌ای با طول‌ها و آرایش مختلف در خاک ماسه‌ای مورد بررسی قرار گرفت. مدل شامل یک فونداسیون به ابعاد ۱۵ × ۱۵ × ۰/۷ متر و شمع‌هایی با قطر متوسط ۱ متر است. زاویه مخروطی ۱/۲۰ درجه منجر به قطرهای بالایی به ترتیب ۱/۲۵، ۱/۳۷۶ و ۱/۵۰۲ متر و قطرهای پایینی ۰/۷۵، ۰/۶۲٤ و ۰/٤۹۸ متر برای طول‌های ۱۲، ۱۸ و ۲٤ متر می‌شود. نرم‌افزار اجزاء محدود پلکسیس سه بعدی برای مدل‌سازی انتخاب شد و از مدل‌های موهر –کلمب و الاستیسته‌ی خطی برای مدل رفتاری خاک و بتن استفاده شد. یک سری تحلیل عددی با تغییر در طول و چیدمان برای شمع‌های استوانه‌ای و مخروطی در رادیه‌ی مربعی انجام شد. نتایج نشان داد که شمع‌های مخروطی باربری جداری بیشتری نسبت به شمع‌های استوانه‌ای دارند. همچنین، رادیه شمع‌های مخروطی نشست تفاضلی کمتری نسبت به رادیه شمع‌های استوانه‌ای از خود نشان دادند.